NASA Technical Memorandum 113085

Tailored Excitation for Multivariable Stability-Margin Measurement Applied to the X-31A Nonlinear Simulation

John T. Bosworth and John J. Burken

August 1997

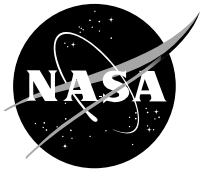

National Aeronautics and
Space Administration

NASA Technical Memorandum 113085

Tailored Excitation for Multivariable Stability-Margin Measurement Applied to the X-31A Nonlinear Simulation

John T. Bosworth and John J. Burken
NASA Dryden Flight Research Center
Edwards, California

1997

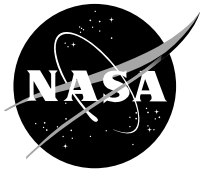

National Aeronautics and
Space Administration

Dryden Flight Research Center
Edwards, California 93523-0273

TAILORED EXCITATION FOR MULTIVARIABLE STABILITY-MARGIN MEASUREMENT APPLIED TO THE X-31A NONLINEAR SIMULATION

John T. Bosworth* and John J. Burken†
NASA Dryden Flight Research Center
Edwards, California

Abstract

Safety and productivity of the initial flight test phase of a new vehicle have been enhanced by developing the ability to measure the stability margins of the combined control system and vehicle in flight. One shortcoming of performing this analysis is the long duration of the excitation signal required to provide results over a wide frequency range. For flight regimes such as high angle of attack or hypersonic flight, the ability to maintain flight condition for this time duration is difficult. Significantly reducing the required duration of the excitation input is possible by tailoring the input to excite only the frequency range where the lowest stability margin is expected. For a multiple-input/multiple-output system, the inputs can be simultaneously applied to the control effectors by creating each excitation input with a unique set of frequency components. Chirp-Z transformation algorithms can be used to match the analysis of the results to the specific frequencies used in the excitation input. This report discusses the application of a tailored excitation input to a high-fidelity X-31A linear model and nonlinear simulation. Depending on the frequency range, the results indicate the potential to significantly reduce the time required for stability measurement.

Nomenclature

Symbols

A	Z transform of the first frequency for the Chirp-Z transform
$f1$	actual lowest frequency in range for excitation, Hz
$f1_D$	desired lowest frequency in range for excitation, Hz
$f2$	actual highest frequency in range for excitation, Hz
$f2_D$	desired highest frequency in range for excitation, Hz
FFT	fast Fourier transformation
G(jω)	plant transfer-function matrix
H(jω)	controller transfer-function matrix
I	identity matrix
j	square root of –1.0
M	the number of points in the time segment input to the Chirp-Z transform
n	index of frequency components in input excitation

*Aerospace Engineer, Controls and Dynamics Branch, 805-258-3792
†Aerospace Engineer, Controls and Dynamics Branch, 805-258-3726

n1	number of cycles of the lowest frequency component in the input excitation signal in the total time to be processed
n2	number of cycles of the highest frequency component in the input excitation signal in the total time to be processed
n_F	number of frequency components in the summed series of cosine waves
RMS	root mean square
s	Laplace operator
t	time, sec
t_P	total time to be processed by the Chirp-Z transform, sec
t_{PD}	total time to be processed by the Chirp-Z transform before rounding to the nearest discrete time interval, sec
u	time series of the experimental excitation input applied to the control-effector actuator, deg
$u1$	time series of the experimental excitation input applied to the first control-effector actuator, deg
$u2$	time series of the experimental excitation input applied to the second control-effector actuator, deg
$u3$	time series of the experimental excitation input applied to the third control-effector actuator, deg
W	multiplying factor to increment frequencies for the Chirp-Z transform algorithm
$w2$	wavelength of highest frequency component in the input excitation signal, sec
$w2_D$	wavelength of highest frequency component in the input excitation signal before adjusting to evenly divide t_P, sec
x	time series of the control system command to the actuator, deg
$x1$	time series of the control system command to the first control-effector actuator, deg
$x2$	time series of the control system command to the second control-effector actuator, deg
Δf	frequency separation between each component of the input excitation signal, Hz
Δt	time separation between points in measured data, sec
ζ	damping ratio of second-order system
μ	singular value
π	the circumference of a circle divided by two times its radius
$\Phi(n)$	Schroeder phase shift to be applied at the nth frequency, rad
ω	frequency, rad/sec

Functions

CEIL	round a real number to the next greatest integer
EXP	inverse of the natural log function
ROUND	round a real number to the nearest integer

Introduction

Safety and productivity of the initial flight test phases of a new vehicle have been enhanced by developing the ability to measure the stability margins of the vehicle in flight.[1–3] The method of measuring stability

of a single feedback path has been extended to analysis of the singular values of a multiple-input/multiple-output system.[4] One shortcoming of performing this analysis is the long duration of the excitation signal (frequency sweep) required to provide results over a relatively wide frequency range. The requirement for a long-duration input was driven by the need to excite the complete frequency range (in particular, the lowest frequencies). In previous applications,[4] the multiple-input/multiple-output system used individual excitation of each loop, which extends the time required for the excitation by the number of control loops times the excitation length. For flight regimes such as high angle of attack and hypersonic flight, the ability to maintain flight condition for this time duration is very difficult, if not impossible.

Flight testing of a new or modified vehicle and flight control system requires an extensive stability-margin survey using the best available models. The data from this analysis provide an expectation of the range of frequencies where the minimum stability margin will occur for specific flight conditions. Although a validation of the frequency response of the system over a wide frequency range is desired, a measurement of the system stability margin only requires excitation across a small range of frequencies. An excitation input can be tailored to excite this specified range of frequencies. Because the excitation signal does not contain frequencies lower than required for stability-margin identification, the length of time for the signal can be minimized. The amount of time saved is increased when the minimum stability margin occurs at a high frequency.

Another means of shortening the excitation time required is to apply an excitation to all of the inputs simultaneously, which can be successfully achieved by designing inputs that are composed of uncorrelated frequency components. Chirp-Z transformation algorithms can be used to match the analysis to the specifically excited frequencies. Similarly, processing time can be reduced by computing singular values only for the specific frequencies.

This report discusses the results obtained when the excitation signal and processing of the results are tailored to obtain a stability margin within a prespecified frequency range. The method is applied to a high-fidelity linear model[5] and nonlinear simulation[6] of the X-31A airplane. The benefits and weaknesses of this technique are discussed.

Approach

A test technique was developed to allow for measuring the stability of a vehicle and flight control system. The objective was to minimize the time required for the input excitation and for processing the results.

Input Excitation Signal Design

A series of summed cosine waves has been shown to provide good excitation over a discrete set of frequencies.[7] A signal with summed cosine waves has the advantage that the dwell time at each frequency is greatly increased in comparison to a frequency-sweep input. By appropriate selection of the discrete frequencies, constructing an input with a period length exactly matching the length of time to be processed is possible. By matching the process time to the period length, problems caused by frequency leakage can be avoided.[8]

For a given desired frequency range of excitation (from $f1_D$ to $f2_D$), the minimum

frequency in the range is the largest contributor to determining the length of the excitation input. To obtain a good estimation of the frequency response in the presence of noise and disturbances, having a time sequence with multiple cycles at the excitation frequency is desired. Experimental results from simulations showed that reasonable results can be obtained with three cycles of excitation. Fewer than three cycles reduces the quality of the results. The maximum desired frequency ($f2_D$) should be adjusted so that it has a period that evenly divides into the total time to be processed (t_P). When $f1_D$ and $f2_D$ are selected, a range of harmonic frequencies between them can be selected such that the cycle lengths divide evenly into t_P. The following logic can be used to construct a series of discrete frequencies for the input excitation signal generation.

Calculate the total time to be processed as n1 cycles of the lowest desired frequency:

$$\mathrm{n1} = 3$$

$$t_{PD} = \mathrm{n1}/f1_D$$

Round this solution to the nearest discrete time step (Δt). The discrete time step Δt is the time between data samples (usually the update rate of the flight control laws):

$$t_P = (\mathrm{ROUND}(t_{PD}/\Delta t)) \times \Delta t$$

The actual starting frequency ($f1$) then becomes:

$$f1 = \mathrm{n1}/t_P$$

The maximum frequency for the excitation is the highest frequency desired adjusted upward so that its wavelength evenly divides the total process time:

$$w2_D = 1/f2_D$$

The actual number of cycles of the ending frequency (n2) and the actual ending frequency ($f2$) are calculated by:

$$\mathrm{n2} = \mathrm{CEIL}(t_P/w2_D)$$

$$f2 = \mathrm{n2}/t_P$$

$$w2 = 1/f2$$

The input excitation can then be generated as a sum of cosines starting with three (n1) wavelengths in t_P and counting up to n2 wavelengths in t_P. The input excitation is normalized by dividing by the total number of frequencies (n_F) to keep the total signal magnitude at approximately 1.0:

$$\mathrm{n_F} = \mathrm{n2} - \mathrm{n1} + 1$$

$$u = \left[\sum_{\mathrm{n}=\mathrm{n1}}^{\mathrm{n2}} \cos(2\pi \times t \times \mathrm{n}/t_P) \right] / \mathrm{n_F}$$

The change in frequency between each component is simply:

$$\Delta f = 1.0/t_P$$

This process generates an excitation (fig. 1) with a desired frequency range from 5.0 to 15.0 rad/sec (n1 = 3, t_P = 3.76, $f1$ = 0.7979 (5.013 rad/sec), $f2$ = 2.3936 (15.040 rad/sec), Δt = 0.02). By using phase shifting as suggested by Schroeder,[7] the following input sum reduces the peak factor of the excitation

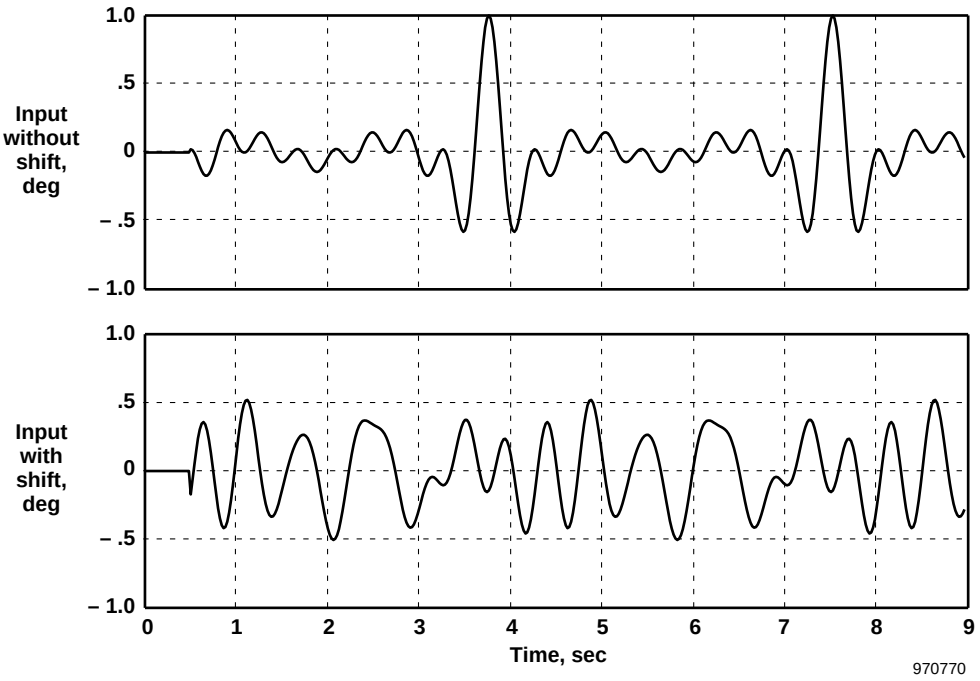

Figure 1. Effect of Schroeder phase shifting on input excitation (n1 = 3, t_P = 3.76, $f1$ = 0.7979 (5.013 rad/sec), $f2$ = 2.3936 (15.040 rad/sec), Δt = 0.02).

while maintaining the same frequency content (fig. 1):

$$\Phi(n) = \pi \times n^2 / n_F$$

$$u = \left[\sum_{n=n1}^{n2} \cos((2\pi \times t \times n / t_p) + \Phi(n)) \right] / n_F$$

The amount of phase shift used at each discrete frequency ($\Phi(n)$) is designed to minimize the overall peak overshoot values.

Matching the Signal Processing to the Excitation

A Chirp-Z transform allows for more flexibility in choosing the frequencies to be processed for a given time segment than a fast Fourier transformation (FFT) algorithm. Using the Chirp-Z transform, the frequencies processed can be matched to those frequencies that comprise the input excitation. The inputs to a Chirp-Z transform algorithm that determine the frequencies processed are as follows:

- The number of points in the time segment (M):

$$M = t_P / \Delta t$$

- The Z transform (or transform into the discrete domain) of the starting frequency (A):

$$A = EXP(j \times 2 \times \pi \times f1 \times \Delta t)$$

- A multiplying factor to increment the subsequent frequencies (W):

$$W = EXP(-j \times 2 \times \pi \times \Delta f \times \Delta t)$$

With these inputs, the first n_F points calculated by the Chirp-Z transform

algorithm correspond to the input excitation frequency components.

Multivariable Stability Analysis

A multiple-input/multiple-output system requires measurement of a set of transfer functions to fully define the dynamic characteristics of the system. This set of transfer functions can be expressed as a complex matrix that varies as a function of frequency. The singular value of this complex matrix is proportional to the minimum perturbation that will cause system instability. Various methods exist for determining the lowest multivariable stability margin of a given system.[9] All of these methods require the measurement of the system dynamics.

This paper addresses the experimental input excitation required to properly measure the system dynamics over a specific frequency range. The reader will have to determine which multivariable stability analysis method should be used to extract margins. A method has been presented for using structured real perturbations that are related directly to individual loop-gain and phase margins.[9] As long as the excitation allows for sufficient identification of the frequency response, the majority of the multivariable stability analysis methods could be applied to the resulting transfer functions.

For the examples presented here, the transfer function $H(j\omega)G(j\omega)/[I + H(j\omega)G(j\omega)]$ was estimated from forced-excitation data. Figure 2 shows the definition of the input and output measurements required to calculate the matrix of closed-loop transfer functions. For simplicity, figure 2 shows a two-input/two-output system. At each frequency, the singular value was computed using complex multiplicative uncertainties.[9] This singular value is plotted as a function of frequency for a given flight condition. The peak value (peak μ) on this plot defines the point of lowest tolerance to multiplicative perturbations at the input to the vehicle dynamics (usually the input to the

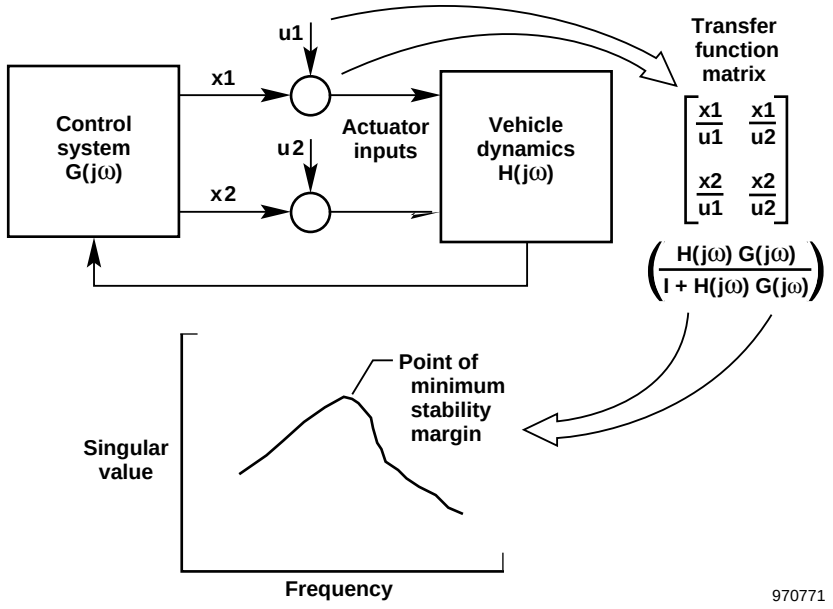

Figure 2. Multivariable stability-margin measurement process.

control-effector actuators).[9] A multivariable stability margin is thus defined for each flight condition, and a specific frequency is identified where the lowest margin is expected to occur.

Simultaneous Excitation

Multivariable stability analysis of experimental data can be performed using separate excitation of each system input to construct a matrix of transfer functions that define the system dynamics.[4] Using separate excitation multiplies the time required for the total excitation by the number of inputs. If a set of uncorrelated excitation signals can be defined, then the signals can be applied to the inputs simultaneously to shorten the total excitation time required.

One method for developing uncorrelated excitation inputs is to use a unique set of frequency components to construct each input. For a case with three control effectors, the input excitation defined in the preceding section can be divided into three separate inputs using the following:

$$u1 = \left[\sum_{n=0}^{n_F/3} \cos((2\pi \times t \times (n1 + 3 \times n)/t_p) + \Phi(n1 + 3 \times n))\right]/(n_F/3)$$

$$u2 = \left[\sum_{n=0}^{n_F/3} \cos((2\pi \times t \times (n1 + 3 \times n + 1)/t_P) + \Phi(n1 + 3 \times n + 1))\right]/(n_F/3)$$

$$u3 = \left[\sum_{n=0}^{n_F/3} \cos((2\pi \times t \times (n1 + 3 \times n + 2)/t_P) + \Phi(n1 + 3 \times n + 2))\right]/(n_F/3)$$

Using this method imposes a requirement that the number of frequencies (n_F) be evenly divisible by the number of inputs (in this case, three). Using the preceding calculation, these three inputs ($u1$, $u2$, and $u3$) are uncorrelated and periodic with a period of t_P. The three resulting excitation inputs are applied simultaneously, and the transfer functions are calculated using Chirp-Z transform algorithms.

The resulting transfer functions obtained from the Chirp-Z transform are valid only for certain discrete frequencies. For example, valid results due to input $u1$ are obtained for frequencies corresponding to index n = 1,4,7,... of the original (undivided) set of frequencies. For each input, the results of the Chirp-Z transform are first thinned to include only results at valid frequency points, then linear interpolation is used to estimate the transfer-function values at the frequencies that were not excited. In this way, a fully populated matrix of transfer functions is approximated over the range of original frequencies. Unless extrapolation is used, the frequency range is reduced by two points at the beginning and ending frequencies. In using this particular method, a multivariable system can be analyzed without the penalty of excitation time required for each individual input.

Application to a Second-Order System

Some of the benefits and areas of concern for using tailored excitation for frequency response identification can be best illustrated with a simple model. The examples presented here use a single-input/single-output second-order system like the one illustrated below:

$$\frac{s + 10.0}{s_2 + 2\zeta 20 + 20^2}$$

Startup Transient Behavior

A stable linear system that is driven by a periodic forcing function over time settles to have a periodic output. Care should be taken to ensure that the data used as input to the Chirp-Z transform are not corrupted by startup transients induced by the application of the excitation input. A system with low damping takes a longer time than a system with high damping for the output to reach a steady-state periodic condition. A system with a low stability margin would be expected to have elements in the transfer-function matrix with low damping. For the purpose of stability-margin measurement, extreme care should be used to ensure that the effect of startup transients does not mask a real stability problem. The input should be applied over a longer time period than is actually processed.

To illustrate one potential effect of a startup transient, a second-order system with damping of ζ = 0.01 was tested. Figure 3 shows the response of this lightly damped system to an input with desired frequencies from 10 to 30 rad/sec (n1 = 5, t_P = 3.14, $f1$ = 1.592 (10.003 rad/sec), $f2$ = 4.777 (30.015 rad/sec), Δt = 0.01). The input was repeated until a steady-state output was achieved (in this case for seven cycles). The resulting output shows that the response approaches a steady-state amplitude by the third cycle. Figure 4 shows the calculated frequency response of the system using only the first cycle compared to using only the third cycle. Results using only the third cycle show greatly improved correlation with the analytic solution.

One means of testing for erroneous results caused by startup transients would be to

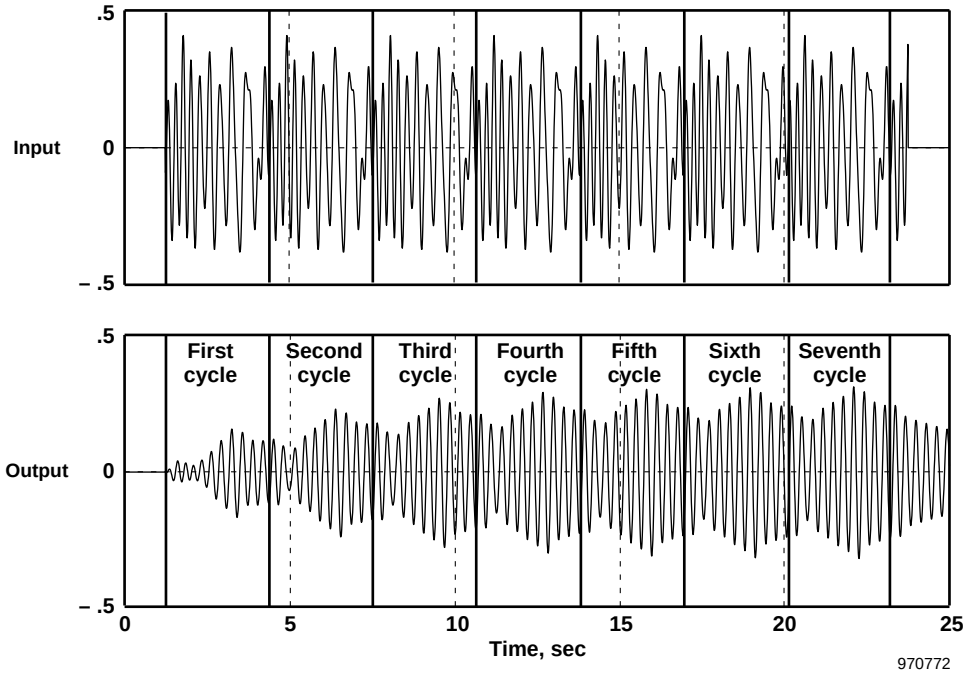

Figure 3. Response of a lightly damped (ζ = 0.01) second-order system to a cyclic tailored excitation (n1 = 5, t_P = 3.14, $f1$ = 1.592 (10.003 rad/sec), $f2$ = 4.777 (30.015 rad/sec), Δt = 0.01).

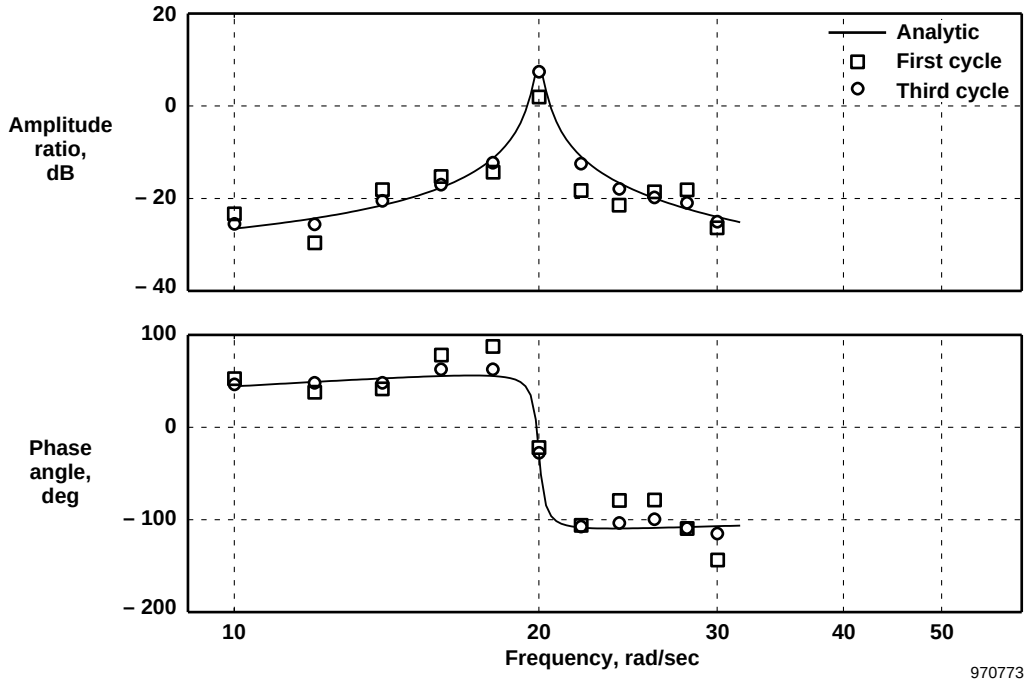

Figure 4. Effect of startup transients on a lightly damped (ζ =0.01) second-order system (n1 = 5, t_P = 3.14, $f1$ = 1.592 (10.003 rad/sec), $f2$ = 4.777 (30.015 rad/sec), Δt = 0.01).

process two segments of data skewed in time. Ideally, the transfer function estimated from these two time segments should be identical. If different results are obtained, it may indicate that a steady-state condition has not been reached. For the extreme case of the lightly damped (ζ = 0.01) second-order system, a test for startup transient errors was devised. The same 3.14-sec period excitation (fig. 3) described in the previous paragraph was used. Multiple time cycles of the input excitation were used to drive the system. Two time segments were processed through the Chirp-Z transform. The two time segments were skewed by one-half of a cycle length (t_P /2). The root mean square (RMS) difference between the magnitude and phase obtained by processing the two segments was calculated.

Table 1 shows the results obtained using various amounts of delay time to allow for startup transients to settle. As would be expected, the RMS errors approached zero as the delay time increased. By choosing an appropriate level of acceptable RMS error, this test can be used with simulation models to determine the amount of time to allow the system to settle to a steady-state

Table 1. Effect of time delay on errors caused by startup transients.

	ζ = 0.01		ζ = 0.02	
Delay time, sec	RMS error amplitude ratio, dB	RMS error phase, deg	RMS error amplitude ratio, dB	RMS error phase, deg
2.0	4.0	28.3	1.88	12.2
4.0	3.6	15.8	1.01	4.32
6.0	1.9	10.2	0.38	1.98
8.0	1.0	8.3	0.13	1.16
10.0	0.8	5.9	0.07	0.52
12.0	0.5	4.2	0.03	0.25

response. In flight test, the RMS error can be calculated to provide some indication of the validity of the calculated margin. For a system with increased damping ($\zeta = 0.02$), the transient effects are much less severe than a system with damping of $\zeta = 0.01$ (table 1).

Further work is needed to refine this validity test. The amount of time skew was chosen somewhat arbitrarily. A large time skew is desired to ensure that steady-state conditions have been reached; however, a large time skew imposes an additional amount of time required for the input excitation. A large time skew also introduces the potential for the flight condition to change. For a specific application, an appropriate time skew would need to be chosen to balance these conflicting requirements.

Frequency Leakage

Frequency leakage occurs when a nonperiodic time segment is processed using Fourier transformations. The Fourier transformation attempts to match a Fourier series to an infinite repetition of the time segment. If the time segment does not start and end with the same value, erroneous results are caused by matching the discontinuity between each time segment. Various windowing techniques are used to minimize the effects of leakage with some success. By using a tailored excitation that forces a periodic system response and matching the length of processed data to the length of the period, frequency leakage can be completely avoided.

Figure 5 shows the effects of frequency leakage when different length time

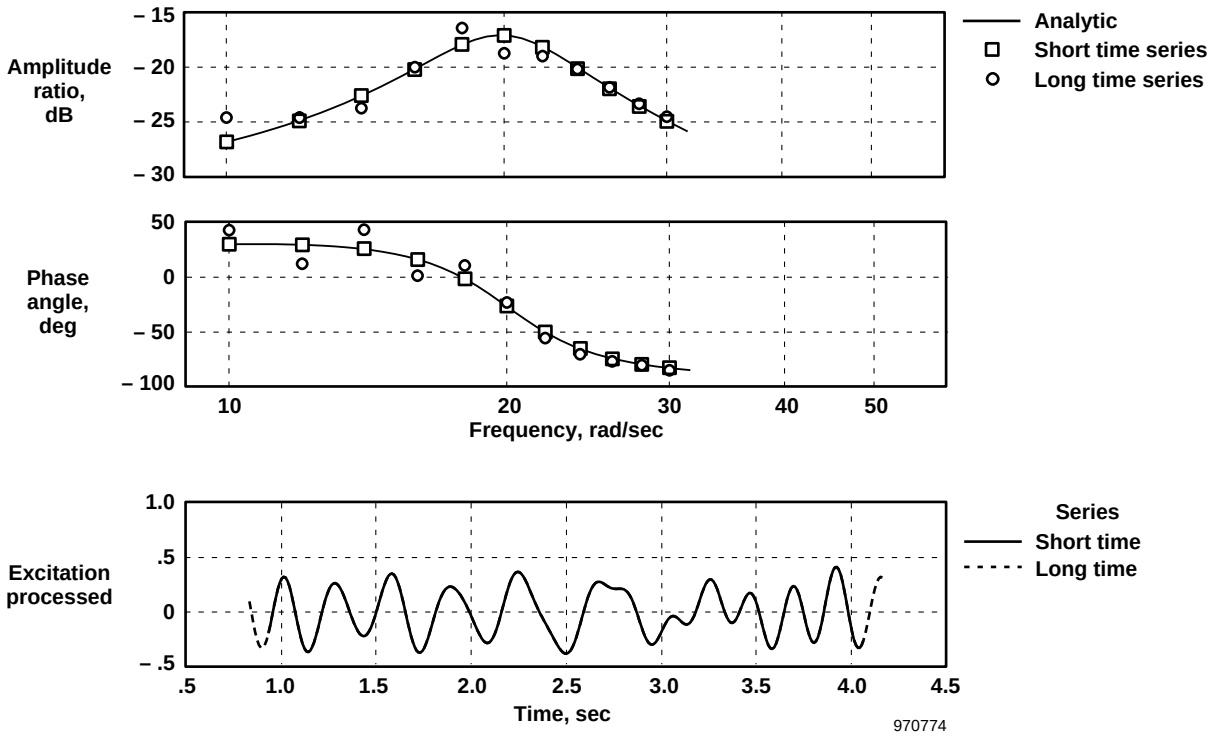

Figure 5. Effect of frequency leakage on a second-order ($\zeta = 0.02$) system (n1 = 5, $t_P = 3.14$, $f1 = 1.592$ (10.003 rad/sec), $f2 = 4.777$ (30.015 rad/sec), $\Delta t = 0.01$).

segments are processed through a Chirp-Z transform. A series of summed cosine waves with a desired frequency range from 10.0 to 30.0 rad/sec (n1 = 5, t_P = 3.14, $f1$ = 1.592 (10.003 rad/sec), $f2$ = 4.777 (30.015 rad/sec), Δt = 0.01) were input to the same second-order filter (described in the Application to a Second-Order System section) with damping of ζ = 0.02. Two different length time segments of the input and output of the filter were processed through a Chirp-Z transform to produce the frequency response of the filter at the excitation frequencies. The length of the short time segment was chosen to match the wavelengths (or some multiple of the wavelengths) of the frequency components of the input excitation (t_P = 3.14). The long time segment used 20 extra time points (t_P = 3.34) and illustrates the erroneous results that can be caused by frequency leakage.

Application to the X-31A Airplane

The X-31A airplane[10] provides an example of an experimental vehicle that initially required an extensive flight envelope clearance process. The X-31A airplane is statically unstable in the longitudinal axis with the worst-case instability of approximately 5 percent mean aerodynamic chord. In the pitch axis, active control of symmetric trailing-edge wing flaps, canards, and pitch thrust vectoring is used for stability and control.[5,10] Although not used for this vehicle, a procedure to measure in flight the multivariable stability margins could have enhanced the efficiency of the flight clearance process.

Definition of Frequency Range

A matrix of 1-g flight conditions (table 2, columns 1–3) was chosen to span the conventional (excluding poststall) flight envelope of the X-31A airplane. A multivariable stability analysis was conducted for the longitudinal axis using multiplicative variations at the input plane (at the actuators). The three inputs (symmetric trailing-edge wing flaps, canards, and pitch thrust vectoring) resulted in a 3-by-3 matrix of transfer functions. Table 2, columns 4 and 5, show the peak singular values (peak μ) and the frequency at which the values occur obtained analytically from a validated, 45-state linear model[5] for each of the flight conditions.

Table 2. Stability margins for the X-31A airplane at selected flight conditions.

Case no.	Altitude, ft	Mach no.	Freq. of peak μ,* rad/sec	Peak μ*	Peak μ†
1	10,000	0.50	1.1	1.42	1.42
2	10,000	0.70	1.5	1.36	1.36
3	10,000	0.90	5.6	1.07	1.06
4	20,000	0.45	1.4	1.30	1.29
5	20,000	0.60	1.4	1.39	1.39
6	20,000	0.80	1.5	1.40	1.40
7	20,000	0.95	4.5	1.11	1.11
8	30,000	0.50	1.0	1.44	1.43
9	30,000	0.70	1.5	1.36	1.35
10	30,000	0.90	3.3	1.15	1.10
11	30,000	1.20	5.6	1.01	0.98

*linear analytic method
†linear time-based method

Figure 6 shows the singular values, obtained analytically from a linear model, plotted as a function of frequency for these flight conditions. As figure 6 and table 2 show, the points of lowest stability (peak μ) occurred in two frequency ranges. Seven cases had minimum margins in the range from 1.0 to 2.0 rad/sec, and four cases (at higher speeds) were within the range from 3.0 to 6.0 rad/sec. Validation of these

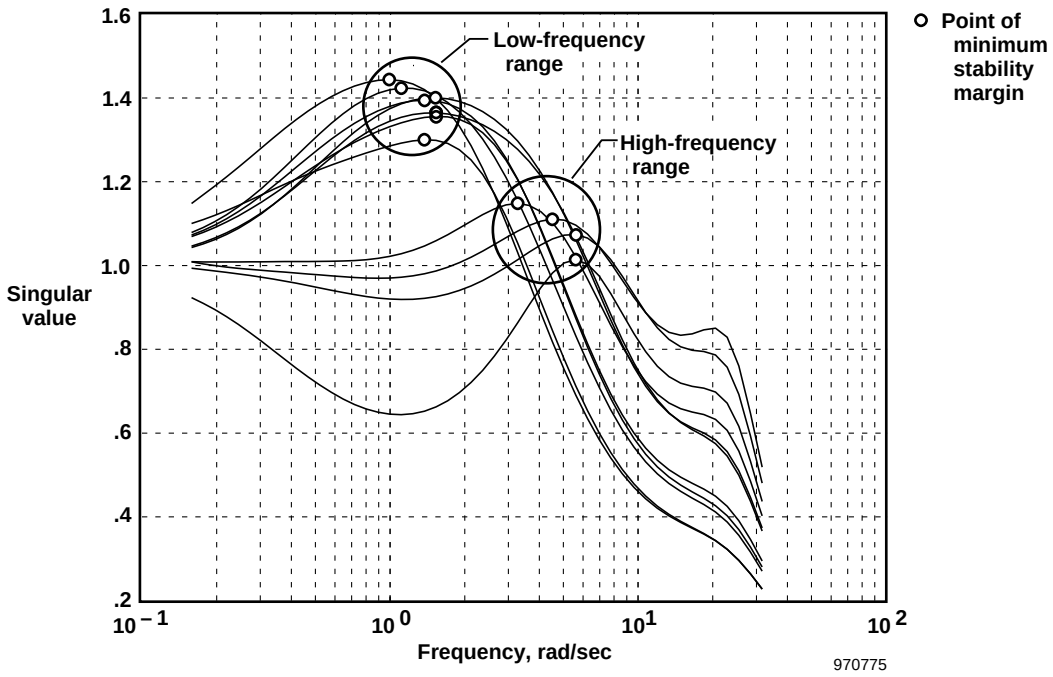

Figure 6. Structured singular values for the X-31A flight envelope.

multivariable stability margins requires excitation and measurement of the dynamics of the vehicle over these two frequency ranges.

Results for the Low-Frequency Range

An excitation signal that covers the frequency range from 0.5 to 3.0 rad/sec was developed to measure the minimum stability margins for seven of the flight conditions shown in table 2. Although the minimum stability margin was expected to occur between 1.0 and 2.0 rad/sec, an extended frequency range was used for two reasons. First, the method using simultaneous inputs without extrapolation results in a reduction in the range of results. Second, differences between predicted and actual (or in this case, between linear and nonlinear) results add some uncertainty in the frequency at which the minimum margin will occur.

Following the procedure proposed in this paper, a tailored excitation input was generated (n1 = 3, t_P = 42.7, $f1$ = 0.0796 (0.500 rad/sec), $f2$ = 0.504 (3.167 rad/sec), Δt = 0.01). A delay of 5 sec was used to avoid startup transient errors. The sum of the total processed time and delay time (45.7 sec) can be compared to more than 120 sec required for FFT analysis with 2048 data points applied to three inputs separately. Because of the low frequencies involved, the majority of the time saving was achieved by using simultaneous inputs rather than by limiting the frequency range.

Figure 7 shows a representative example comparing the results from linear analytic methods with the time-domain approach using the linear model at Mach 0.7 and an altitude of 10,000 ft (case 2). Columns 5 and 6 in table 2 show results using the linear model with both analytical and time-domain methods for each of the flight

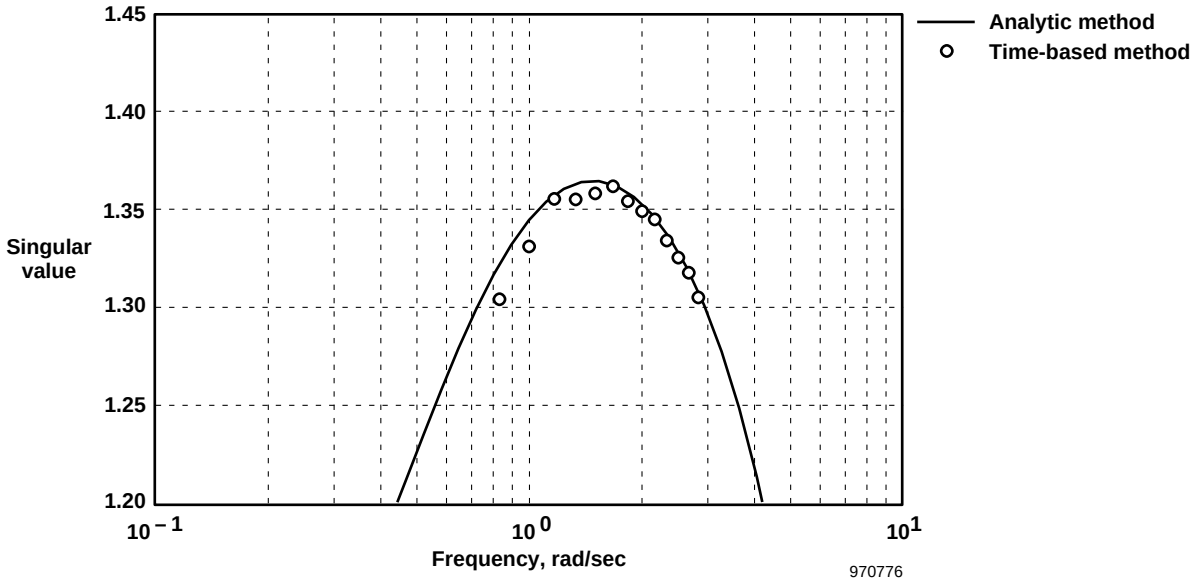

Figure 7. Structured singular values for the linear model of the X-31A airplane at Mach 0.70 and an altitude of 10,000 ft (case 2, n1 = 3, t_P = 42.7, $f1$ = 0.0796 (0.500 rad/sec), $f2$ = 0.504 (3.167 rad/sec), Δt = 0.01).

conditions. In general, excellent correlation exists between the time-domain and analytical methods.

The same tailored input (with the exception that Δt = 0.02) was applied to the X-31A nonlinear simulation[6] at Mach 0.7 and an altitude of 10,000 ft (case 2) (table 2). Figure 8 shows results from analytic linear analysis as well as time-based results from the nonlinear simulation using simultaneous inputs and long (2048-point) Schroeder inputs applied separately to each control input. The results using long, separately applied inputs are included as the "truth" model for the nonlinear simulation. Differences exist between the linear and nonlinear results. Some portion of this difference is a result of the simplifying assumptions that were used to formulate the linear model.

The results using simultaneous inputs fall between the results from linear analysis and the nonlinear simulation that used separate inputs. Both of the time-based analysis methods produce somewhat erratic results. The low frequencies involved are on the lower edge of the frequency range over which good results can be obtained. The difficulty stems from the requirement for a long-duration input that does not cause the vehicle to change flight condition. In addition, the technique that used long Schroeder inputs applied separately showed a sensitivity to the time duration of the applied input in relation to the sample time processed. This sensitivity indicates a frequency leakage problem. Another contributor to the erratic nature of the data obtained with time-based methods seems to be an accumulated effect of relatively small numerical errors in each of the nine transfer-function estimations used in the computation of the singular value.

All three methods predicted a peak magnitude on the singular value plot within

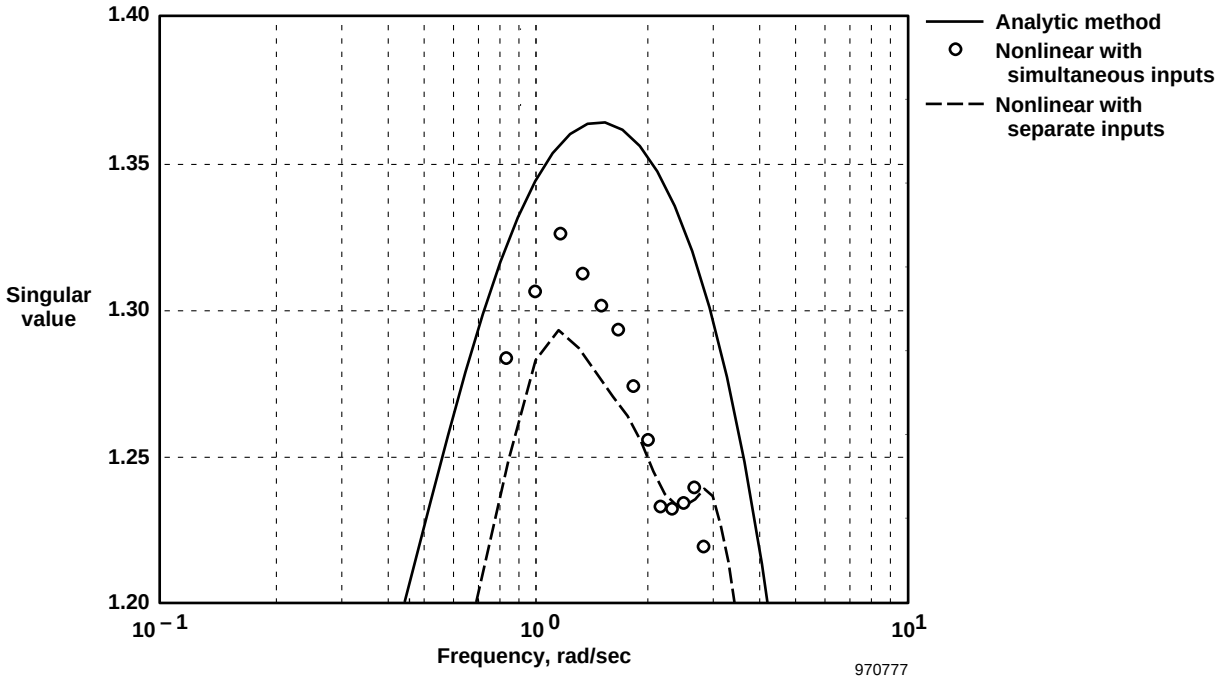

Figure 8. Structured singular values of the X-31A airplane at Mach 0.70 and an altitude of 10,000 ft (case 2) using the nonlinear simulation and compared to analytic results (n1 = 3, t_P = 42.7, $f1$ = 0.0796 (0.500 rad/sec), $f2$ = 0.504 (3.167 rad/sec), Δt = 0.02).

approximately 5 percent of the lowest peak value. The frequency at which the peak occurs correlates well for all three methods. The results from the tailored excitation input provide a reasonable measure of the stability margin of the system.

Results for the High-Frequency Range

All of the cases where the minimum stability margin fell within the high-frequency range were high-speed cases. For the X-31A airplane, the thrust-vectoring system is not used at high dynamic-pressure flight conditions, which simplifies the problem for these cases to a 2-by-2 matrix of transfer functions. In addition, the high-frequency range from 2.0 to 10.0 rad/sec allows for a much shorter duration excitation signal than the low-frequency range allows. Following the procedure proposed in this paper, a tailored excitation input was generated (n1 = 3, t_P = 9.42, $f1$ = 0.3185 (2.001 rad/sec), $f2$ = 1.5924 (10.005 rad/sec), Δt = 0.01). A delay of 5 sec was used to avoid startup transient errors. The sum of the total processed time and delay time (14.42 sec) can be compared to more than 82 sec required for FFT analysis with 2048 data points applied to two inputs separately.

Figure 9 shows a comparison of linear analysis with the time-domain approach at Mach 0.9 and an altitude of 10,000 ft (case 3). Columns 5 and 6 in table 2 show results using the linear model with both analytic and time-domain solutions for each of the flight conditions. For the linear model, good correlation exists between the time-based and analytical methods.

The same inputs (with the exception that Δt = 0.02) were applied to the nonlinear simulation at Mach 0.9 and an altitude of 10,000 ft (case 3). Figure 10 shows

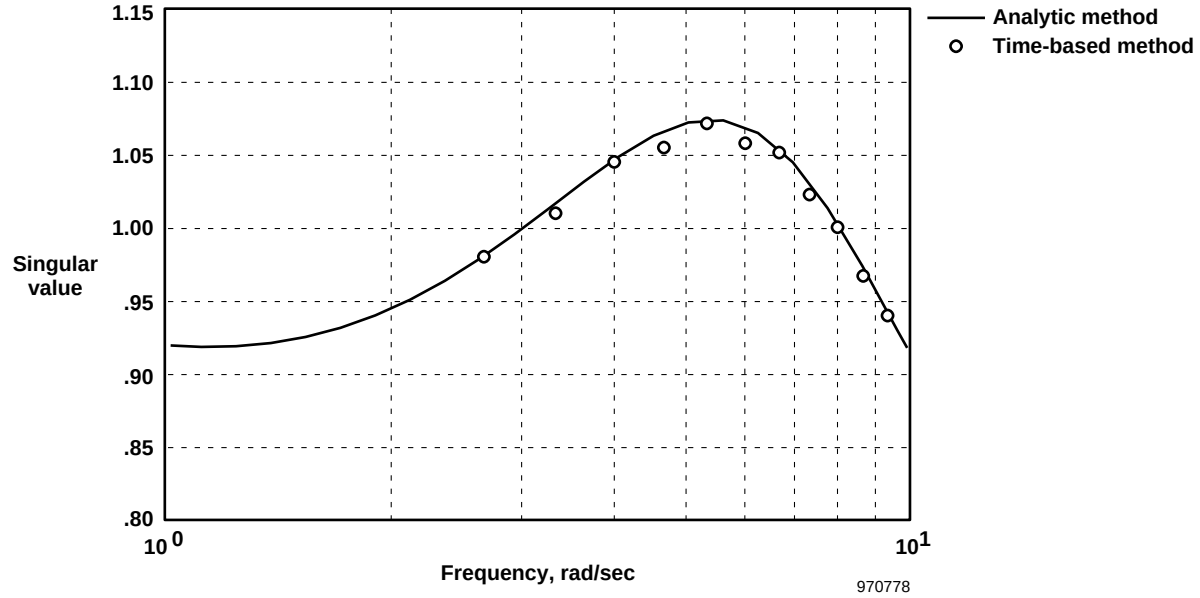

Figure 9. Structured singular values for the linear model of the X-31A airplane at Mach 0.90 and an altitude of 10,000 ft (case 3, n1 = 3, t_P = 9.42, $f1$ = 0.3185 (2.001 rad/sec), $f2$ = 1.5924 (10.005 rad/sec), Δt = 0.01).

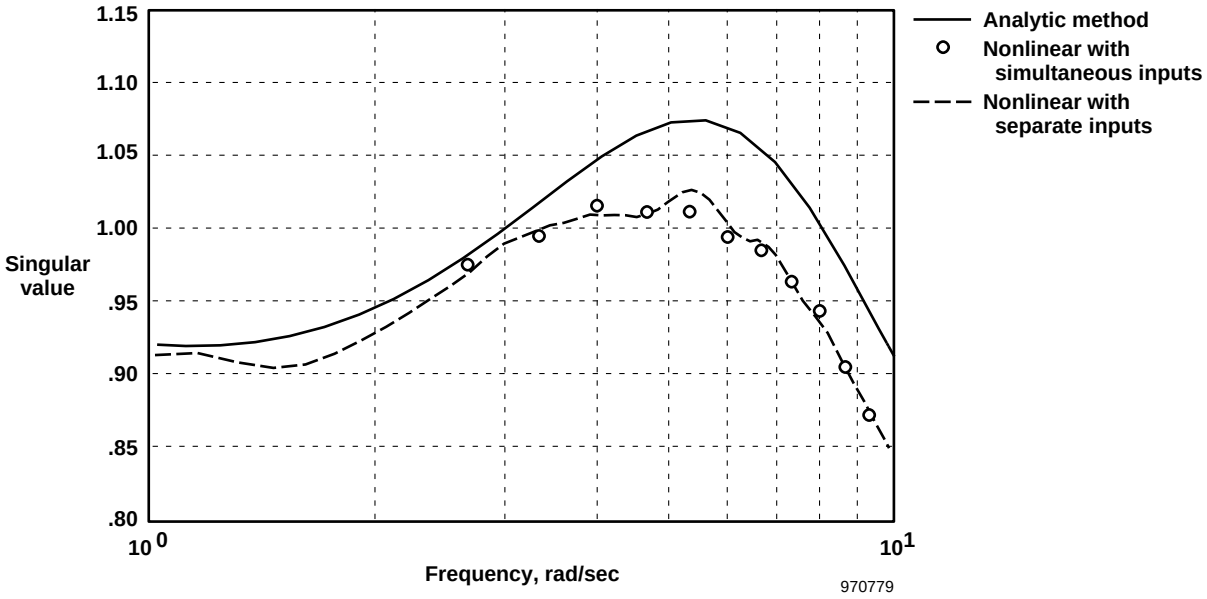

Figure 10. Structured singular values of the X-31A airplane at Mach 0.90 and an altitude of 10,000 ft (case 3) using the nonlinear simulation and compared to analytic results (n1 = 3, t_P = 9.42, $f1$ = 0.3185 (2.001 rad/sec), $f2$ = 1.5924 (10.005 rad/sec), Δt = 0.02).

results from linear analysis and the nonlinear simulation using simultaneous inputs and long (2048-point) Schroeder inputs applied separately to each control input. As in the comparison for case 2, figure 10 shows differences between the linear and nonlinear results.

For this case, the results obtained using separate inputs correlate better with the results from simultaneous inputs when compared to the low-frequency data. Also for case 3, both of the time-based analysis methods provide less erratic results compared to case 2. These improved results could be caused in part by a reduction in the number of elements in the transfer-function matrix (four for a 2-by-2 matrix as opposed to nine for a 3-by-3 matrix). However, FFT analysis generally provides better results for this frequency range compared to the low range.

All three methods predicted a peak magnitude on the singular value plot within approximately 7 percent of the lowest peak value. Because of the relatively flat nature of the peak magnitude, the frequency at which the peak occurs did not correlate as well as for the low-frequency range. All three methods showed a peak within the range of frequencies analyzed.

Concluding Remarks

An experimental method was developed to shorten the time required for in-flight stability-margin measurement. This method is proposed for applications where long-duration inputs are not practical. The method relies on a good prediction of the frequency range where the minimum stability margin occurs.

Savings in the time required to obtain stability-margin measurements were achieved by combining a tailored excitation input with Chirp-Z transformation algorithms and focusing the data processing on a specific frequency range. Increased time savings were achieved in the case where the minimum stability margin occurred in the high-frequency range (3–6 rad/sec). In addition, results for a multivariable system were obtained by simultaneously applying uncorrelated inputs, resulting in further savings in the required time for the input excitation.

A Schroeder wave input was used to excite a particular set of discrete frequencies to cover the range where the minimum stability margin of a system was expected to occur. The lowest frequency in the range defines the length of excitation signal required. For the cases examined here, three cycles of the lowest frequency were found to provide sufficient excitation to use for the frequency-response calculation algorithm.

Each frequency component of the tailored input excitation was chosen so that an integer number of cycles occurred within the time length to be processed. This method ensured that the problems associated with frequency leakage could be avoided.

For systems with low damping, significant errors could be introduced if the system was not allowed to reach a steady-state periodic condition. A delay was added between the excitation application and the sampling of the results. A proposed test for errors induced by startup transients was devised; however, further testing is needed to ensure that the time required for this test does not conflict with the short time required for transitory flight conditions.

The experimental method produced a reasonable measurement of the stability margin of the system when compared to linear analysis. The method was applied to both a high-order linear model and nonlinear simulation of the X-31A vehicle.

For the X-31A airplane, the minimum stability margin occurred within two frequency ranges, depending on the flight condition. The high-frequency range allowed for a greater reduction in input excitation time than the low-frequency range allowed. Results from the low-frequency range were somewhat erratic (not smooth). The low frequencies involved and consequent long-duration inputs tend to cause changes in flight condition that corrupt the results. The tailored excitation input demonstrated less susceptibility to frequency leakage problems when compared to results from long-duration Schroeder inputs.

The approach outlined in this paper provides an experimental method with the potential for measuring stability margins for vehicles at flight conditions (high angles of attack or hypersonic accelerating flight) where long periods at steady-state are difficult, if not impossible, to achieve. Further proof of the concept in the flight environment is warranted.

References

[1]Bosworth, J. T. and J. C. West, “Real-Time Open-Loop Frequency Response Analysis of Flight Test Data,” AIAA-86-9738, Apr. 1986.

[2]Gera, J., “Dynamics and Controls Flight Testing of the X-29A Airplane,” AIAA-86-0167, Jan. 1986.

[3]Gera, J., J. T. Bosworth, and T. H. Cox, *X-29A Flight Test Techniques and Results: Flight Controls*, NASA TP-3121, 1991.

[4]Burken, J. J., “Flight-Determined Multivariable Stability Analysis and Comparison of a Control System,” *AIAA Journal of Guidance, Control, and Dynamics*, vol.16, no. 6, Nov.–Dec. 1993, pp. 1026–1031.

[5]Stoliker, P. C., John T. Bosworth, and Jennifer Georgie, “Linearized Poststall Aerodynamic and Control Law Models of the X-31A Airplane and Comparison with Flight Data,” NASA-TM-4807, 1997.

[6]Norlin, Ken A., *Flight Simulation Software at NASA Dryden Flight Research Center*, NASA TM-104315, 1995.

[7]Flower, J. O., G. F. Knott, and S. C. Forge, “Application of Schroeder-Phased Harmonic Signals to Practical Identification,” *Journal of Measurement and Control*, vol. 11, no. 2, Feb. 1978, pp. 69–73.

[8]Schoukens, J., Rik Pintelon, Edwin Van Der Ouderaa, and Jean Renneboog, “Survey of Excitation Signals for FFT Based Signal Analyzers,” *IEEE Transactions on Instrumentation and Measurement*, vol. 37, no. 3, Sept. 1988, pp. 342–352.

[9]Miotto, P. and J. Paduano, “Application of Real Structured Singular Values to Flight Control Law Validation Issues,” AIAA-95-3190, Aug. 1995.

[10]Beh, H. and G. Hoffinger, “X-31A Control Law Design,” AGARD-CP-548, Mar. 1994, pp. 13-1–13-9.

REPORT DOCUMENTATION PAGE

Form Approved
OMB No. 0704-0188

1. AGENCY USE ONLY (Leave blank)	2. REPORT DATE	3. REPORT TYPE AND DATES COVERED
	August 1997	Technical Memorandum

4. TITLE AND SUBTITLE

Tailored Excitation for Multivariable Stability-Margin Measurement Applied to the X-31A Nonlinear Simulation

5. FUNDING NUMBERS

WU-529-30-04

6. AUTHOR(S)

John T. Bosworth and John J. Burken

7. PERFORMING ORGANIZATION NAME(S) AND ADDRESS(ES)

NASA Dryden Flight Research Center
P.O. Box 273
Edwards, California 93523-0273

8. PERFORMING ORGANIZATION REPORT NUMBER

H-2197

9. SPONSORING/MONITORING AGENCY NAME(S) AND ADDRESS(ES)

National Aeronautics and Space Administration
Washington, DC 20546-0001

10. SPONSORING/MONITORING AGENCY REPORT NUMBER

NASA TM-113085

11. SUPPLEMENTARY NOTES

Presented at the Society of Flight Test Engineers Conference, Orlando, Florida, August 18–22, 1997.

12a. DISTRIBUTION/AVAILABILITY STATEMENT

Unclassified—Unlimited
Subject Category 08

12b. DISTRIBUTION CODE

13. ABSTRACT (Maximum 200 words)

Safety and productivity of the initial flight test phase of a new vehicle have been enhanced by developing the ability to measure the stability margins of the combined control system and vehicle in flight. One shortcoming of performing this analysis is the long duration of the excitation signal required to provide results over a wide frequency range. For flight regimes such as high angle of attack or hypersonic flight, the ability to maintain flight condition for this time duration is difficult. Significantly reducing the required duration of the excitation input is possible by tailoring the input to excite only the frequency range where the lowest stability margin is expected. For a multiple-input/multiple-output system, the inputs can be simultaneously applied to the control effectors by creating each excitation input with a unique set of frequency components. Chirp-Z transformation algorithms can be used to match the analysis of the results to the specific frequencies used in the excitation input. This report discusses the application of a tailored excitation input to a high-fidelity X-31A linear model and nonlinear simulation. Depending on the frequency range, the results indicate the potential to significantly reduce the time required for stability measurement.

14. SUBJECT TERMS

Control, Excitation, Fourier, Margin, Stability

15. NUMBER OF PAGES

21

16. PRICE CODE

AO3

17. SECURITY CLASSIFICATION OF REPORT	18. SECURITY CLASSIFICATION OF THIS PAGE	19. SECURITY CLASSIFICATION OF ABSTRACT	20. LIMITATION OF ABSTRACT
Unclassified	Unclassified	Unclassified	Unlimited